IEICE TRANS. COMMUN., VOL.E92–B, NO.3 MARCH 2009

PAPER

Turbo Equalization of Nonlinear TDMA Satellite Signals

Yen-Chih CHEN[†a)], *Student Member and* **Yu Ted SU**[†], *Nonmember*

SUMMARY In this paper, we investigate a coded solution to compensate for the nonlinear distortion of TDMA satellite waveforms. Based on a Volterra-type channel model and the turbo principle, we present a turbo-like system that includes a simple rate-1 encoder at the transmit side in addition to a conventional channel encoder; the receive side iteratively equalizes the nonlinear channel effect and decodes the received symbols. Some other design alternatives are also explored and computer simulated performance is presented. Numerical results show that significant improvement over conventional approaches can be achieved by the proposed turbo system.

key words: *Volterra series, turbo equalizer, nonlinear channel*

1. Introduction

To make efficient use of the digital satellite communication spectrum through the sharing of a single transponder by several earth stations accessing it, robust and highly bandwidth/power efficient transmission techniques such as time division multiple access (TDMA) with phase shift keying (PSK) or constant envelop modulations are often employed. The desire to maximize downlink power output often necessitates a satellite high power amplifier (HPA) to be driven at or near saturation. However, operating at or close to the saturation point inevitably introduces nonlinear distortions [1]. An appropriate input back-off (IBO) is thus needed to guarantee that the transponder's HPA operates in the linear region, leading to output (downlink) power loss [2].

In order to increase output power efficiency of the available HPA power, several techniques were proposed to compensate for the nonlinear satellite channel effect. Three approaches, namely, data pre-distortion [4], analog pre-distortion [5], [6] and nonlinear equalization [7], [8], have been considered. The first approach attempts to modify the data constellation before modulation. The second approach performs signal pre-distortion in pass-band while the third approach tries to equalize the nonlinear effect at the receiving end. In this paper, we present a new solution that belongs to the third class.

Characterization of the nonlinear satellite channels by Volterra series models was first suggested by Benedetto, Biglieri and Daffara [9]. Although a Volterra model with long memory requires high computing and memory complexity, equalization of satellite signals based on Volterra series, however, has been proven to benefit from their inherent relatively short memory [8]. Nonlinear Volterra equalizer followed by a maximum-likelihood sequence detection (MLSD) receiver can thus provide an effective solution that balances system performance and computational complexity.

Turbo equalization techniques, which was first proposed in [10], have received considerable attention for their excellent performance and are successfully applied in equalizing linear dispersive channels. We present an iterative joint equalization and decoding technique for nonlinear satellite channels [20]. Regarding the nonlinear satellite channel as a finite-state machine, we apply the so called turbo-principle to iteratively equalize the nonlinear channel effect based on some known soft-input soft-output (SISO) algorithms.

The following section introduces a discrete-time Volterra model for typical satellite TDMA channels, defines the corresponding parameters and then presents a nonlinear finite-state Markov model. Section 3 proposes solutions for compensating the nonlinear effect, suggesting a pre-coding architecture and a turbo equalization method. Section 4 gives some simulated bit error probability behavior of the proposed solutions while the last section summarizes our findings.

2. Modeling and Identification of TDMA Satellite Channels

An HPA like traveling-wave-tube amplifier (TWTA) is often modelled as a frequency independent memoryless bandpass nonlinearity and can be completely characterized by the corresponding AM/AM and AM/PM conversion curves [11]. For the HPA input signal

$$x(t) = r(t)\cos[\omega_0 t + \varphi(t)], \tag{1}$$

where ω_0 is the carrier frequency, $r(t)$ and $\varphi(t)$ are the associated envelope and phase, respectively, the corresponding output waveform can be written as

$$y(t) = A[r(t)]\cos\{\omega_0 t + \varphi(t) + \Phi[r(t)]\}, \tag{2}$$

where $A(r)$ represents the AM/AM conversion and $\Phi(r)$ describes the AM/PM conversion.

Saleh [11] showed that $A(r)$ and $\Phi(r)$ can usually be closely approximated by substituting appropriate parameter values into

Manuscript received February 18, 2008.
Manuscript revised September 27, 2008.

[†]The authors are with the Department of Communications Engineering, National Chiao Tung University, 1001 Dar Hsueh Rd., Hsinchu, 30056, Taiwan.
a) E-mail: joechen.cm88g@nctu.edu.tw

DOI: 10.1587/transcom.E92.B.992

$$A(r) = \frac{\alpha_a r}{(1+\beta_a r^2)} \tag{3}$$

and

$$\Phi(r) = \frac{\alpha_\phi r^2}{(1+\beta_\phi r^2)}. \tag{4}$$

Typically, the AM/AM conversion distorts the input signal waveform, while the AM/PM conversion introduces different time delay for each input power level. Furthermore, although the AM/AM and AM/PM conversions are memoryless, the linear filters prior to and after an HPA make the combined nonlinear satellite channel one with memory.

Let $\mathbf{a}_k = [a_k, a_{k+1}, a_{k+2} \cdots a_{k+L}]^T$ be a transmitted data sequence, where T denotes vector transposition and L is the channel memory length. The discrete-time sequence at the output of a ground receiver matched filter, $\{y_k\}$, can be expressed as

$$y_k = g(\mathbf{a}_k) + n_k \tag{5}$$

where $g(\cdot)$ represents the combined nonlinear channel effect that includes transmit pulse shaping filter, pre-filter, onboard high power amplifier (HPA), post-filter, and receive matched filter (see Fig. 3), n_k is the noise component which consists of thermal noise and, perhaps, jamming and other radio frequency interference. A well known model for a nonlinear channel with memory $\tilde{y}_n \stackrel{def}{=} f(\mathbf{a}_n)$ is the Volterra model

$$\tilde{y}_n = h_0 + \sum_{i=0}^{N-1} h_1(i) a_{n-i} + \sum_{i=0}^{N-1}\sum_{j=0}^{N-1}\sum_{k=0}^{N-1} h_3(i,j,k) a_{n-i} a_{n-j} a^*_{n-k} + \cdots \stackrel{def}{=} f(a_n, a_{n-1}, \cdots, a_{n-N+1}) \tag{6}$$

where $h_1(\cdot)$, $h_3(\cdot), \cdots$ are the Volterra kernels of the nonlinear channel. $f(a_n, a_{n-1}, ..., a_{n-N+1})$ is used to emphasize that the channel output is a function of $a_n, \cdots a_{n-N+1}$. Note that due to the bandpass nature of the satellite channel, only odd-order terms appear in (6). Furthermore, if a constant envelope waveform like PSK is used, some of the coefficients in (6) can be combined. For example, the third-order Volterra model requires 31 coefficients, including the dc term h_0, three linear coefficients, and twenty-seven third-order cross product terms. But the fact that, for PSK signals, $a_n a^*_n$ is a constant for all n reduces the number of coefficients to 22.

The set of coefficients can be identified by the setup shown in Fig. 1 where an adaptive algorithm is used to minimize the mean squared error

$$e_k = y_k - \tilde{y}_k = [g(\mathbf{a}_k) - f(\mathbf{a}_k)] + n_k. \tag{7}$$

Figure 2 plots the LMS-based learning curve of the identification setup of Fig. 1 for two typical sets of parameters [11], indicating good approximation of the Volterra model. The identification process is assumed to be carried out at ground (before the satellite transponder is put on board) so that the link noise can be ignored. We discuss the effect of link noise in Sect. 4 when the identification process is performed in real time and the satellite is already in its designated orbital position.

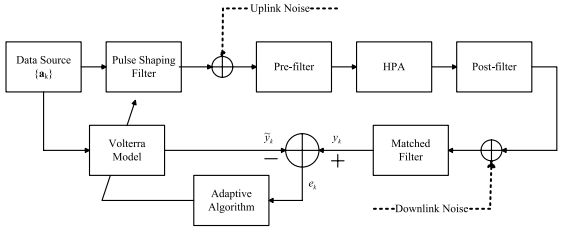

Fig. 1 A satellite communication channel identification setup. The data source output refers to the ground transmitter's encoder output while the channel output is at the ground receiver's matched filter output. Inputs from the dotted lines are included in the setup only if the link noise is present.

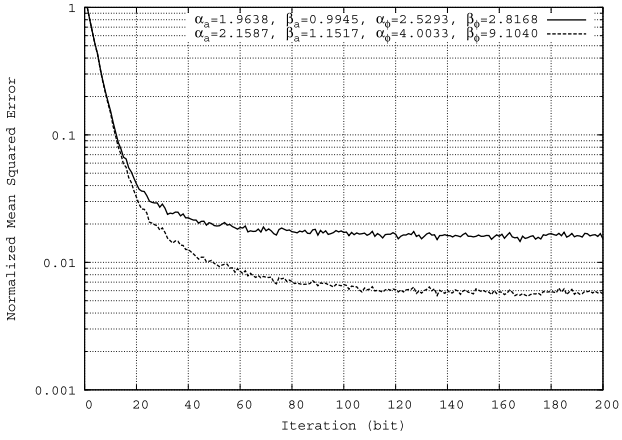

Fig. 2 Learning curves of LMS-based channel identification process; step size $\mu = 0.002$.

The discrete-time input-output relation of a Volterra channel can be written in a more compact vector form

$$\tilde{y}_k = f(\mathbf{a}_k) = \mathbf{h}^T \mathbf{a}_{aug,k}, \tag{8}$$

where $\mathbf{a}_{aug,k}$ is the augmented data vector, $\mathbf{a}^T_{aug,k} = [1,\ a_k,\ a_{k-1},\ a_{k-2},\ a_k a_k a^*_{k-1},\ a_k a_k a^*_{k-2},\ \ldots]$ and $\mathbf{h}$ is the coefficients vector associated with $f(\mathbf{a}_k)$. One can express the nonlinear function $f(\mathbf{a}_k)$ as $f(a_k, \rho_k)$, where $\rho_k = (a_{k-1}, a_{k-2}, \cdots, a_{k-L})$ represents the channel state at time k and L is the channel memory order. This expression implies that the channel input-output relation can be described by a nonlinear finite-state machine (FSM). This model differs from the conventional FSM for linear systems or linear codes in that the range of the nonlinear function f is not the same as its domain (usually a set of finite alphabets) but a complex combination of input alphabets and their cross products of various orders. With a QPSK sequence as the input, the behavior of the output of a nonlinear channel of memory order two can be completely described by a 16-state Markov chain.

3. Combined Equalization and Decoding

In the above section, we show that a satellite channel can

be described by a nonlinear convolutional-like encoder. For a coded satellite link, the 'channel' between the uplink encoder input and the ground receiver's matched filter output can thus be regarded as a serial concatenated coded system. In such a system, an interleaver is often placed at the output of the (inner) error-correcting encoder so that the input to the outer-code decoder is corrupted by random independent errors only. On the other hand, without an interleaver, one can also regard the combined inner and outer codes as a single composite code and, at the expense of an increasing complexity, perform maximum likelihood decoding of the received sequence accordingly.

However, the presence of an interleaver facilitates the utilization of the iterative (turbo) processing technique that repeats the equalization and decoding procedures based on the same set of received data and a companion set of evolving extrinsic information that is updated at both the equalizer and decoder outputs. The feedback information from the decoder is interleaved and passed to the equalizer and a so-called interleaving gain can thus be obtained. It was shown in [12] that a more significant interleaving gain is possible for a serial concatenated convolutional code if and only if the inner encoder is recursive. [13] shows that a significant performance gain can be achieved by placing a rate-1 recursive pre-coder in front of the channel. Since the Volterra model represents a non-recursive encoder, to improve the interleaving gain, we use a scheme similar to that of [14], inserting a rate-1 pre-coder at the output of the interleaver so that the resulting 'channel' becomes a recursive inner code; see Fig. 3. Note that the rate-1 pre-coder does not change the memory length of the channel whence will neither increase the decoding complexity nor decrease the data rate.

A block diagram of the complete system, including a recursive equalizer-decoder, is shown in Fig. 3. The equivalent inner code that represents the channel effect between the pre-coder input and receiver complex matched filter output is a nonbinary complex code while the outer code we use is a binary convolutional code. For a QPSK uplink signal, we need conversion rules between 4-ary and binary symbols to provide soft output values during each decoding iteration.

Let $P_r(a_t, \mathbf{y})$ be the joint probability density function (pdf) of a received sequence $\mathbf{y}$ and a complex QPSK symbol $a_t = (a_t^0, a_t^1)$ at time t where a_t^0, a_t^1 are the corresponding real and imagine parts, respectively. After employing the BCJR algorithm to obtain $P_r(a_t, \mathbf{y})$, the *a posteriori* log-likelihood ratio (LLR) of the interleaved coded bits $\{a_t^i\}_{i=0,1}$ is given by

$$\Gamma_i(a_t^i) = \log \frac{P_r(a_t^i = +1|\mathbf{y})}{P_r(a_t^i = -1|\mathbf{y})} = \log \frac{\sum\limits_{a_t:\ a_t^i=+1} P_r(a_t|\mathbf{y})}{\sum\limits_{a_t:\ a_t^i=-1} P_r(a_t|\mathbf{y})}. \quad (9)$$

The summation in (9) is taken over all QPSK input symbols whose ith bit is $+1$ or -1. Notice that such a conversion is equivalent to regarding the portion of the satellite link between the interleaver output and the nonlinear channel output as a (nonlinear) binary-input complex-output code so that algorithms for decoding serially concatenated binary codes can be easily modified to serve the current application. The corresponding soft output (extrinsic value) can thus be derived from computing the LLR of a conventional binary code. In computing $P_r(a_t, \mathbf{y})$ and the corresponding log-likelihood, the nonlinear metric $m(y_t, a_t) \stackrel{def}{=} |y_t - f(a_t + a_{t-1}, \rho_t)|^2$ is used, where the sum $a_t + a_{t-1}$ represents the precoding effect.

Let $\Gamma_{ie}(c_{t,j})$ be the extrinsic information associated with the interleaved coded bit $c_{t,j}$ obtained in the course of decoding the inner code and is based on the received vector along with the interleaved extrinsic information provided by the outer code decoder from the previous iteration, $\overline{\Gamma}_{oe}(\tilde{c}_{t,j})$. Note that the notations "$-$" and "$\sim$" represents the operations of interleaving and deinterleaving respectively. Thus $\tilde{c}_{t,j}$ is the deinterleaved coded bit that corresponds to $c_{t,j}$. This information is to be calculated by [15]

$$\Gamma_{ie}(c_{t,j}) = \Gamma_i(c_{t,j}) - \overline{\Gamma}_{oe}(\tilde{c}_{t,j}) \quad (10)$$

where $c_{t,j}$ is the corresponding jth interleaved coded bit that results in the transition from state at $(t-1)$ to state at t. Note that in our setup $c_{t,j} = a_t^j$, $j = 0, 1$, and the output likelihood ratio $\Gamma_i(c_{t,j})$ of the equalizer (inner decoder) is thus equivalent to $\Gamma_i(a_t^j)$.

The input *a priori* information of the inner code, $\overline{\Gamma}_{oe}(\tilde{c}_{t,j})$, is obtained by interleaving the channel (equivalent outer) code decoder output $\Gamma_{oe}(\tilde{c}_{t,j})$. $\overline{\Gamma}_{oe}(\tilde{c}_{t,j})$ has an initial value of zero as the outer decode has not yet been activated. The soft output of the outer decoder is composed of the deinterleaved extrinsic information, $\widetilde{\Gamma}_{ie}(c_{t,j})$, from the inner code and the extrinsic information $\Gamma_{oe}(\tilde{c}_{t,j})$ to be sent to the inner code for next iteration decoding, i.e.

$$\Gamma_o(\tilde{c}_{t,j}) = \widetilde{\Gamma}_{ie}(c_{t,j}) + \Gamma_{oe}(\tilde{c}_{t,j}). \quad (11)$$

Based on the extrinsic information of the outer code bits, the priori symbol probability used in the MAP decoding procedure of the inner code (equalizer) is then given by

$$P_r(a_t = \alpha_p) = \prod_{j=0}^{1} P_r(c_{t,j} = \beta_{p,j}) \quad (12)$$

where $\{\beta_{p,j}\}_{j=0}^1$ is mapped to symbol α_p, which is drawn from the finite alphabet set of QPSK. The bit probability in (12) can be derived from the interleaved extrinsic information of the outer decoder. That is,

$$\begin{aligned} P_r(c_{t,j} = \beta_{p,j}) &= \begin{cases} \frac{\exp[\overline{\Gamma}_{oe}(\tilde{c}_{t,j})]}{1+\exp[\overline{\Gamma}_{oe}(\tilde{c}_{t,j})]}, & \text{for } \beta_{p,j} = 1 \\ \frac{1}{1+\exp[\overline{\Gamma}_{oe}(\tilde{c}_{t,j})]}, & \text{for } \beta_{p,j} = -1 \end{cases} \\ &= \frac{1}{2}\left[1 + \beta_{p,j} \tanh\left(\frac{1}{2}\overline{\Gamma}_{oe}(\tilde{c}_{t,j})\right)\right]. \end{aligned} \quad (13)$$

4. Simulation Results and Discussion

This section reports some simulated performance of the proposed turbo equalizer as well as that of some other schemes

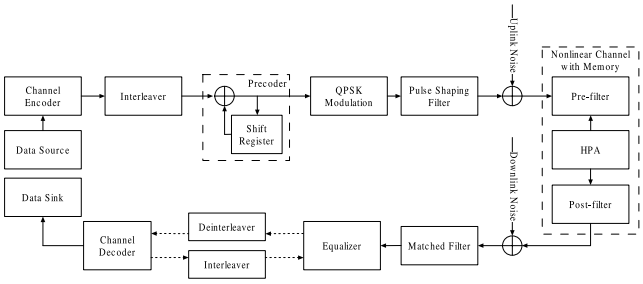

Fig. 3 Functional block diagram of a complete satellite link that uses an iterative equalizer-decoder (turbo equalizer).

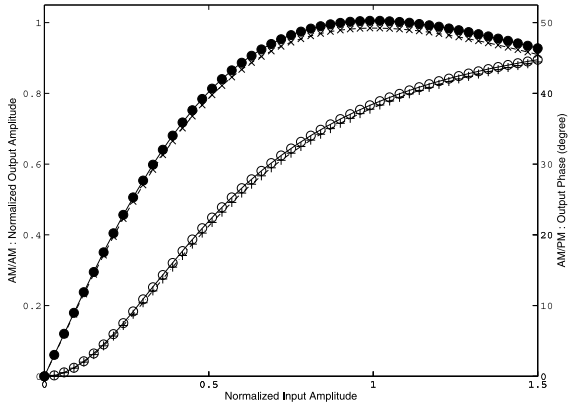

Fig. 4 AM/AM and AM/PM conversion characteristics for the TWTA with (a) $\alpha_a = 2.01056, \beta_a = 2.36786, \alpha_\phi = 6.32325, \beta_\phi = 7.0420$ ($-\bullet-, -\circ-$), and (b) $\alpha_a = 1.9638, \beta_a = 0.9945, \alpha_\phi = 2.5293, \beta_\phi = 2.8168$ ($-\times-, -+-$) [11].

for comparison. Our simulation is based on the system block diagram of Fig. 3 in which the QPSK modulation is used. A square root raised cosine filter with a roll-off factor 1 is used for pulse shaping. Both the pre- and post-filters are the fifth-order Chebyshev filter with a 3-dB cutoff frequency of 0.75 R_s, where $R_s = \frac{1}{T}$ is the symbol rate. 0 dB input backoff is assumed. The binary channel encoder is a rate-1/2 convolutional code and we use a pseudo-random interleaver with a size equals to the length of a TDMA slot. The same interleaver/deinterleaver pair is assumed for all simulations. Details of the equalizer shown in Fig. 3 are described in Sect. 3. An (n, m, K) convolutional code is referred to as a convolutional code with code rate $\frac{m}{n}$ and constraint length K, where the constraint length is defined as the maximum number of bits in a single output stream that can be affected by any input bit. Moreover, the (2,1,3) and (2,1,7) codes used have generator polynomials $[1 + D^2,\ 1 + D + D^2]$ and $[1 + D^2 + D^3 + D^5 + D^6,\ 1 + D + D^2 + D^3 + D^6]$ respectively, and the receiver employs an iterative Log-MAP decoding rule. The length of the training sequence is 100 bits. We also assume that the uplink SNR is high enough that the associated noise effect can be ignored.

The nonlinear models (3) and (4) with parameters $\alpha_a = 2.01056$, $\beta_a = 2.36786$, $\alpha_\phi = 6.32325$ and $\beta_\phi = 7.0420$ are used to simulate the HPA operation. The TWTA's output saturation point corresponds to an input amplitude of

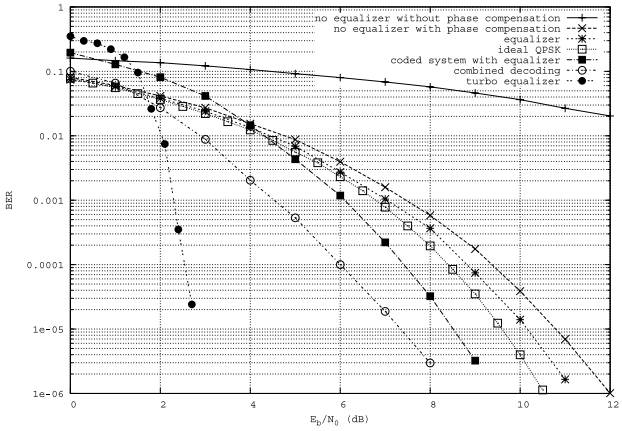

Fig. 5 Performance of several coded and uncoded satellite TDMA systems.

0.65, which matches to the average input power to the TWTA when the modulator output envelop is normalized to 1. Figure 4 illustrates the AM/AM and AM/PM conversions. After input normalization, the characteristic of the TWTA model used is almost identical to that used in [11], i.e., $\alpha_a = 1.9638$, $\beta_a = 0.9945$, $\alpha_\phi = 2.5293$ and $\beta_\phi = 2.8168$, which were obtained by curve-fitting some experimental TWTA data.

Figure 5 compares the performance of various system configuration scenarios. We consider (i) conventional uncoded receiver without phase compensation (+), (ii) conventional uncoded receiver with phase compensated ($\times$) [17], (iii) uncoded system with ML equalizer based on the Volterra model ($*$), (iv) (2,1,3) convolutional coded system with ML equalizer followed by conventional hard-decision decoder (■), (v) (2,1,3) convolutional coded system with combined ML equalization and decoding without interleaver ($\circ$), and (vi) coded system with turbo equalization ($\bullet$). Performance of the ideal uncoded QPSK receiver ($\square$) is also given for convenience of comparison. For the system of (vi), we assume an interleaver of size 1024 and 4 decoding iterations. These curves indicate that when $\frac{E_b}{N_0}$ is greater than 1.8 dB, iterative ("turbo") equalization method yields the best performance.

In Fig. 6, we compare the performance of two binary convolutional codes. The iteration number used in this simulation is 4. Although the (2,1,7) code has a larger free distance, the (2,1,3) code has a smaller number of low-weight codewords (error coefficient). As was shown in [16], the turbo decoder performance at low $\frac{E_b}{N_0}$'s is dominated by the error coefficient. We also notice that the (2,1,7)-coded system tends to outperform the other system when $\frac{E_b}{N_0} > 3.5$ dB.

The impacts of interleaving size and the number of iterations are shown in Figs. 7 and 8. As expected, increasing the interleaving size leads to better BER performance. In contrast to parallel-concatenated turbo codes, the proposed turbo equalizer does not result in an error floor at high $\frac{E_b}{N_0}$ within the range of interest. Further convergence analysis can be explored from the use of EXIT chart proposed in [18]. The complete system consists of a rate-1, 16-state re-

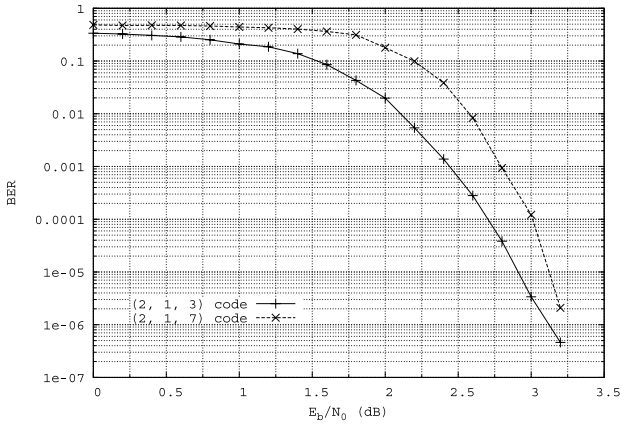

Fig. 6 Bit error probability performance of the proposed turbo equalizer for two different convolutional codes; 4 iterations.

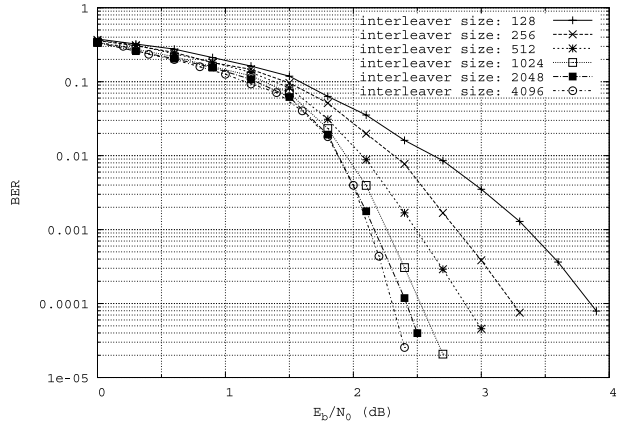

Fig. 7 Influence of the interleaving size on the BER performance of the turbo equalized system; 4 iterations.

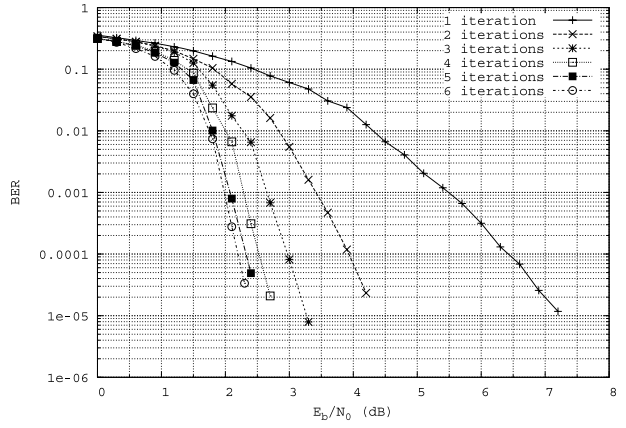

Fig. 8 Effect of the decoding iteration number on the BER performance of the turbo equalized system; interleaving size = 1024.

cursive nonsystematic convolutional code as the inner code and a rate $\frac{1}{2}$, 4-state feed-forward convolutional code as the outer code, yielding an overall code rate of $\frac{1}{2}$. Figure 8 indicates that, for an interleaving size of 1024, there is only limited improvement for iterations greater than 4.

Figure 9 plots the BER performance of different input

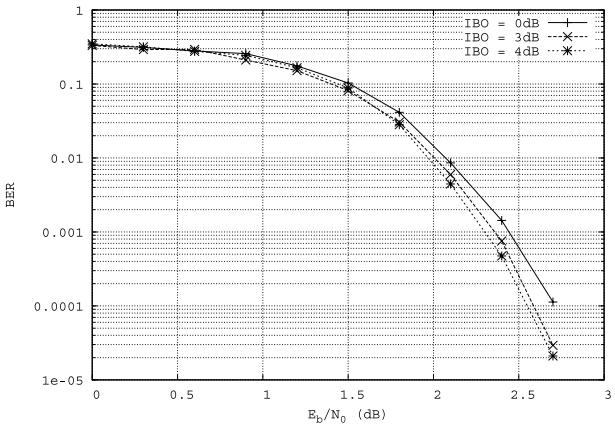

Fig. 9 BER performance for different IBO values; step size $\mu = 0.004$.

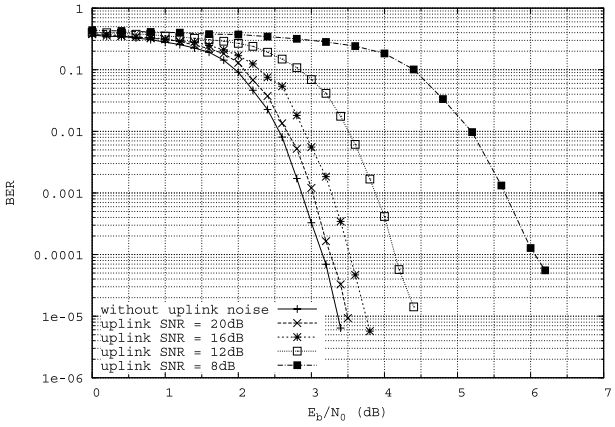

Fig. 10 Effects of the uplink noise, downlink noise and identification errors on the BER performance of the turbo equalized system; interleaving size = 1024, step size $\mu = 0.001$.

power backoff (IBO) values for the turbo equalized system of Fig. 3. The input power backoff is defined as, IBO $\stackrel{def}{=} \frac{A_{sat}^2}{P_{in}}$, where A_{sat} is the input saturation point of TWTA and P_{in} is the average power of input signal. These performance curves reveal that most of the nonlinear channel distortion has been effectively mitigated by the proposed turbo equalizer and increasing IBO brings about only minor BER performance improvement; very little performance gain is obtained for IBO greater than 3 dB. Although increasing the IBO improves the BER performance, larger IBO also introduces more total degradation (TD), which is defined as the sum (in decibels) of increase SNR due to nonlinearity and the output power backoff (OBO) [19]. Since only small IBO is needed for the proposed system, we avoid introducing large TD while guaranteeing a desired reception quality.

Figure 10 plots the BER performance for the case that the Volterra model coefficients are estimated in the presence of uplink and downlink AWGN noise with the channel identification setup of Fig. 1. We assume that the system identification process is carried out in real-time using a training sequence. The results indicate that identification with a noisy input leads to less accurate FSM model whence less

satisfactory system performance especially when the uplink SNR is smaller than 12 dB. Compared with the zero-uplink-noise performance, the performance loss at BER=10^{-5} is less than 0.5 dB if the uplink SNR is larger than 16 dB. Our numerical experiments also reveal that the step size used in the LMS model identification algorithm has a profound impact on the model accuracy and therefore the turbo equalizer's performance. The step size 0.001 used in Fig. 10 is a near optimal one. If a step size of 0.004 is used instead the resulting performance will become much worse.

5. Conclusion

We have examined several detection alternatives for receiving nonlinear TDMA satellite waveforms. We extend the turbo equalization concept used for combating linear dispersive channels to the class of nonlinear satellite channels. Computer simulation gives numerical performance that is consistent with our prediction. That is, the proposed turbo equalization solution that performs iterative joint equalization and decoding based on a Volterra model does offer excellent performance. A simple identification setup is given and two scenarios for obtaining the model coefficients are considered and their impacts on the system performance are examined. We also find that a judicious choice of the channel code is important especially in low SNR environments. Finally, our numerical study indicates that, for the TDMA/QPSK system under consideration, an interleaving size of 1024 with four decoding iterations is an appropriate design choice.

References

[1] D. Chakraborty, T. Noguchi, S.J. Campanella, and C.J. Wolejsza, "Digital modem design for nonlinear satellite channels," 4th Int. Conf. Digital Satellite Commun., Montreal, P.Q., Canada, 1978.
[2] R.M. Gagliardi, Introduction to Communications Engineering., John Wiley & Sons, 1988.
[3] D. Roddy, Satellite Communications., Prentice Hall, Englewood Cliffs, 1989.
[4] A.A.M. Saleh and J. Salz, "Adaptive linearization of power amplifiers in digital radio systems," Bell Syst. Tech. J., vol.62, no.4, pp.1019–1033, April 1983.
[5] J. Namiki, "An automatically controlled predistorter for multilevel quadrature amplitude modulation," IEEE Trans. Commun., vol.31, no.5, pp.707–712, May 1983.
[6] S. Pupolin and L.J. Greenstein, "Performance analysis of digital radio links with nonlinear transmit amplifiers," IEEE J. Sel. Areas Commun., vol.5, no.3, pp.534–546, April 1987.
[7] M.F. Mesiya, P. McLane, and L.L. Campbell, "Maximum likelihood sequence estimation of binary sequences transmitted over bandlimited nonlinear channels," IEEE Trans. Commun., vol.25, no.7, pp.633–643, July 1977.
[8] S. Benedetto and E. Biglieri, "Nonlinear equalization of digital satellite channels," IEEE J. Sel. Areas Commun., vol.1, no.1, pp.57–61, Jan. 1983.
[9] S. Benedetto, E. Biglieri, and R. Daffara, "Modeling and performance evaluation of nonlinear satellite links-A Volterra series approach," IEEE Trans. Aerosp. Electron. Syst., vol. AES-15, no.4, pp.494–507, July 1979.
[10] C. Douillard, M. Jezequel, C. Berrou, A. Picart, P. Didier, and A. Glevieux, "Iterative correction of intersymbol interference: Turbo equalization," Eur. Trans. Telecommun., vol.6, no.5, pp.507–511, Sept.-Oct. 1995.
[11] A.A.M. Saleh, "Frequency-independent and frequency-dependent nonlinear models of TWT amplifiers," IEEE Trans. Commun., vol.COM-29, no.11, pp.1715–1720, Nov. 1981.
[12] S. Benedetto, D. Divsalar, G. Montorsi, and F. Pollara, "Serial concatenation of interleaved codes: Design and performance analysis," IEEE J. Sel. Areas Commun., vol.16, pp.186–195, Feb. 1998.
[13] I. Lee, "The effect of a precoder on serially concatenated coding systems with an ISI channel," IEEE Trans. Commun., vol.49, no.7, pp.1168–1175, July 2001.
[14] K.R. Narayanan, U. Dasgupta, and B. Liu, "Low complexity turbo equalization with binary precoding," Proc. IEEE ICC'2000, vol.1, pp.1–5, 2000.
[15] B. Vucetic and J. Yuan, Turbo codes: Principles and applications, Kluwer, 2000.
[16] J. Yuan, B. Vucetic, and W. Feng, "Combined turbo codes and interleaver design," IEEE Trans. Commun., vol.47, no.4, pp.484–487, April 1999.
[17] A. Gutierrez and W.E. Ryan, "Performance of Volterra and MLSD receivers for nonlinear band-limited satellite systems," IEEE Trans. Commun., vol.48, no.7, pp.1171–1177, July 2000.
[18] S. ten Brink, "Designing iterative decoding schemes with the extrinsic information transfer chart," AEÜ Arch. Elektron. Übertragung., vol.54, no.6, pp.289–298, Dec. 2000.
[19] A.N. D'Andrea, V. Lottici, and R. Reggiannini, "RF power amplifier linearization through amplitude and phase predistortion," IEEE Trans. Commun., vol.44, no.11, pp.1477–1484, Nov. 1996.
[20] Y.T. Su, M.-C. Chiu, and Y.-C. Chen, "Turbo equalization of nonlinear TDMA satellite signals," Proc. IEEE GLOBECOM, vol.3, pp.2860–2864, Nov. 2002.

Yen-Chih Chen received the B.S. degree in control engineering from National Chiao Tung University, Hsinchu, Taiwan, R.O.C., in 1996, and the M.S. degree in electrical engineering in National Taiwan University of Science and Technology, Taipei, Taiwan, R.O.C., in 1999. He is now a Ph.D. candidate in the Department of Communication Engineering of National Chiao Tung University. His main research interests include communication theory and statistical signal processing.

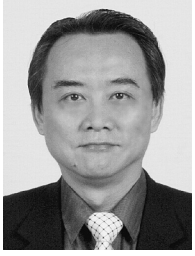

Yu Ted Su received the B.S.E.E. degree from Tatung Institute of Technology, Taipei, Taiwan and the University of Southern California, Los Angeles, USA, in 1974 and 1983, respectively. From 1983 to 1989, he was with Lin-Com Corporation, Los Angeles, USA, where his last position was a Corporate Scientist. Since September 1989, he has been with the National Chiao Tung University, Hsinchu, Taiwan, where he was an Associative Dean of the College of Electrical and Computer Engineering from 2004–2007, Head of the Communications Engineering Department from 2001 to 2003. He is also afliated with the Microelectronic and Information Systems Research Center of the same university and served as a Deputy Director from 1997 to 2000. In 2005, he was appointed as the Area Coordinator of National Science Council's Telecommunications Programme. His main research interests include communication theory and statistical signal processing.